Colloids and Surfaces B: Biointerfaces 162 (2018) 380–388

Contents lists available at ScienceDirect

Colloids and Surfaces B: Biointerfaces

journal homepage: www.elsevier.com/locate/colsurfb

Study of non-covalent interactions on dendriplex formation: Influence of hydrophobic, electrostatic and hydrogen bonds interactions

María Sánchez-Milla[a,b,c], Isabel Pastor[c,d], Marek Maly[e], M. Jesús Serramía[c,f,g,h], Rafael Gómez[a,b,c], Javier Sánchez-Nieves[a,b,c,*], Félix Ritort[c,d], M. Ángeles Muñoz-Fernández[c,f,g,h], F. Javier de la Mata[a,b,c,*]

[a] Department of Química Orgánica y Química Inorgánica, Universidad de Alcalá (IRYCIS), Campus Universitario, E-28871 Alcalá de Henares, Madrid, Spain
[b] Instituto de Investigación Química "Andrés M. del Río" (IQAR), Universidad de Alcalá, Spain
[c] Networking Research Center on Bioengineering, Biomaterials and Nanomedicine (CIBER-BBN), Madrid, Spain
[d] Small Biosystems Lab, Condensed Matter Physics Department, Universitat de Barcelona, C/Martí i Franquès, E-08028, Barcelona, Spain
[e] Faculty of Science, J. E. Purkinje University, Ceske mladeze 8, 400 96 Usti nad Labem, Czech Republic
[f] Sección Inmunología, Laboratorio de InmunoBiología Molecular, Hospital General Universitario Gregorio Marañón, Madrid, Spain
[g] Instituto de Investigación Sanitaria Gregorio Marañón, Madrid, Spain
[h] Spanish HIV HGM BioBank, Madrid, Spain

ARTICLE INFO

Article history:
Received 5 August 2017
Received in revised form
10 November 2017
Accepted 7 December 2017
Available online 8 December 2017

Keywords:
Dendrimers
Carbosilane
Gene therapy
siRNA
Molecular dynamics
Force spectroscopy

ABSTRACT

The interaction of a double stranded small interference RNA (siRNA Nef) with cationic carbosilane dendrimers of generations 1–3 with two different ammonium functions at the periphery ($[-NMe_2R]^+$, R = Me, $(CH_2)_2OH$) has been studied by experimental techniques (zeta potential, electrophoresis, single molecule pulling experiments) and molecular dynamic calculations. These studies state the presence of different forces on dendriplex formation, depending on generation and type of ammonium group. Whilst for higher dendrimers electrostatic forces mainly drive the stability of dendriplexes, first generation compounds can penetrate into siRNA strands due to the establishment of hydrophobic interactions. Finally, in the particular case of first generation dendrimer $[G_1O_3(NMe_2(CH_2)_2OH))_6]^{6+}$; the presence of hydroxyl groups reinforces dendriplex stability by hydrogen bonds formation. However, since these small dendrimers do not cover the RNA, only higher generation derivatives protect RNA from degradation.

1. Introduction

Gene therapy is a technique that uses genetic material, such as plasmids, nucleic acids (DNA and RNA) and oligonucleotides, to treat diseases and has become a very attractive research area [1]. However, the aforesaid naked systems are easily degraded and also are unable to penetrate into the cells due to their size and negative charge. To circumvent this problem, gene delivery carriers have been developed. The mission of these vectors is to turn nucleic acid invisible to nucleases and favour the crossing of cell membranes. Two types of gene delivery vectors can be distinguished: viral and non-viral. Viruses and their modifications show considerable disadvantages due to their nature [2,3]. On the other hand, non-viral vectors are synthetic systems, such as macromolecules, polymers and nanosystems, being designed by controlled procedures [4–11]. These carriers interact with nucleic acids, usually electrostatically, compacting them and preventing their degradation. For this reason, an important type of nucleic acid vectors are cationic macromolecules [12]. Another important factor in the design of synthetic vectors is the size of the nucleic acid to transfect, from small oligonucleotides to the biggest DNA, requiring bigger delivery systems as the size of the nucleic acid increases. Hence, since cationic systems are toxic, a higher charge number leads to higher toxicity and, therefore, it is desirable to find smaller carriers while keeping an adequate activity.

Dendrimers are spherical macromolecules with well-defined size and structure, monodisperse, flexible, and with a multivalent molecular surface, that have attracted attention for biomedical applications [13–19]. Several types of cationic dendrimers con-

* Corresponding authors at: Department of Química Orgánica y Química Inorgánica, Universidad de Alcalá (IRYCIS), Campus Universitario, E-28871 Alcalá de Henares, Madrid, Spain
E-mail addresses: javier.sancheznieves@uah.es (J. Sánchez-Nieves), javier.delamata@uah.es (F.J. de la Mata).

https://doi.org/10.1016/j.colsurfb.2017.12.009
0927-7765/

taining different skeletons have been explored for gene therapy, based on the multicationic charge on their surface [6,10,20–28]. One important advantage of these systems is that their controlled synthesis minimizes structural defects and allows establishing structure-activity relationships more easily than for classical polymeric materials. However, several important drawbacks are the intrinsic toxicity of cationic macromolecules, and in the case of dendrimers, also the number of reaction steps necessary and time-consuming for their synthesis, mainly if high generation dendrimers are prepared. Thus, the synthesis of bigger dendrimers usually introduces more defects in their structure. With the aim to shorten synthesis, several accelerated procedures have been developed [29,30], including the use of click-chemistry [31,32].

Carbosilane dendrimers are one type of dendrimers with a framework made of C—C and Si—C bonds that generates highly hydrophobic systems [33]. However, if the periphery contains charged groups, these dendrimers present an amphiphilic behaviour that differentiates them from other kinds of dendrimers with a more hydrophilic skeleton. Thus, low generation cationic dendrimers and dendrons present important bactericide ability [34,35] and facilitate the trespassing of blood brain barrier [36–38]. Regarding their use as non-viral vectors for gene therapy, cationic carbosilane dendrimers bind oligonucleotides and siRNA, protect the nucleic material from degradation and transport them to the interior of a range of cell types [36,39–46]. However, one of the more active systems as gene carriers contains water unstable Si—O bonds that make difficult their widespread use [41], whereas an analogous compound, containing two ammonium groups per branch, with stable Si—C bonds was very inactive due to difficulties for nucleic acid release [47].

Considering these previous results, we believe that an important improvement in dendrimers applicability is not only the synthesis simplification but also modification of interactions between dendrimers and targets. For example, some groups have shown the relevance of the dendrimer skeleton in the activity, while keeping the number and type of peripheral functional groups [48], or the topology of dendrimer in the activity [49]. Regarding cationic systems, the hiding of charges or incorporation of lipophilic moieties in hydrophilic structures reduce toxicity and increase activity [50–53]. Our group has explored modifications in the peripheral cationic surface that could diminish the charge effect while maintaining an adequate interaction with nucleic acids [36], or also combining carbosilane and pegylated fragments to form a Janus type dendrimer improving interaction with RNA with respect to fully carbosilane system [46].

We have also reported that the presence of hydroxyethylene moieties in cationic dendrimers of the type $[G_nO_3(NMe_2((CH_2)_2OH)_m]^{m+}$ reduces slightly the surface charge, with respect to related $[G_nO_3(NMe_3)_m]^{m+}$, whilst the hydroxyl groups are available for interaction with other molecules [34]. Continuing with these studies, in this work we describe the influence of the ammonium groups $[-NMe_2R]^+$ (R = Me, $(CH_2)_2OH$) of dendrimers $[G_nO_3(NMe_2R)_m]^{m+}$ in the formation of dendriplexes with siRNA Nef. This small interference RNA is the antisense sequence that codifies HIV Nef protein, which interacts with the cell surface proteins favoring HIV infection. Formation of dendriplexes has been evaluated by Z potential and electrophoresis assays and the stability has been studied by molecular modeling. This last methodology is well stablished and widely used to provide important information about the interaction between dendrimers/polymers and nucleic acids [54–58]. Moreover we have carried out single molecule force spectroscopy studies of two types of such dendrimers interacting with an RNA model hairpin to evaluate their binding affinity. Our study emphasizes the relevance of different interactions between dendrimers and siRNA: hydrophilic (electrostatic), hydrophobic and hydrogen bonding. Finally, assays regarding stability of dendriplexes and their inhibition efficacy have been carried out.

2. Materials and methods

2.1. Synthesis and characterization of dendrimers

Compounds $HS(CH_2)_2NMe_2{\cdot}HCl$, 2,2′-dimethoxy-2-phenylacetophenone (DMPA), MeI, $I(CH_2)_2OH$, $HSiMeCl_2$, 1,3,5-$(HO)_3C_6H_3$, K_2CO_3, were obtained from commercial sources. Compounds $[G_nO_3(NMe_2)_m]$ and $[G_nO_3(NMe_2R)_m(I)_m]$ (n = 1, m = 6; n = 2, m = 12; n = 3, m = 24; R = Me (**1-3**), $(CH_2)_2OH$ (**4-6**))[34] were synthesized as published, except first generation derivatives that were prepared following a modification that is described in Supporting Information. All reactions were carried out under inert atmosphere and solvents were purified from appropriate drying agents when necessary. Thiol-ene reactions were carried out employing a HPK 125 W mercury lamp from Heraeus Noblelight with maximum energy at 365 nm, in normal glassware under an inert atmosphere. NMR spectra were recorded on a Varian Unity VXR-300 (300.13 (^{1}H), 75.47 (^{13}C) MHz) or on a Bruker AV400 (400.13 (^{1}H), 100.60 (^{13}C), 40.56 (^{15}N), 79.49 (^{29}Si) MHz). Chemical shifts (δ) are given in ppm. ^{1}H and ^{13}C resonances were measured relative to internal deuterated solvent peaks considering TMS = 0 ppm, meanwhile ^{15}N and ^{29}Si resonances were measured relative to external MeNO and TMS, respectively. When necessary, assignment of resonances was done from HSQC, HMBC, COSY, TOCSY and NOESY NMR experiments. Elemental analyses were performed on a LECO CHNS-932. Mass Spectra were obtained from a Bruker Ultraflex III and an Agilent 6210.

2.2. siRNA

All siRNA sequences were chosen by previously published results [41,59,60] and had inhibited HIV replication in experiments using transiently transfected cells. They were purchased from Dharmacon. Inc. (Lafayette, CO). The sequence of the siRNA NEF was, sense: GUGCCUGGCUAGAAGCACAdTdT, antisense: UGUGCUUCUAGCCAGGCACdTdT. The siNEF labeled with the fluorochrome cyanine 3 (Cy3) on the 5′ end of the sense strand was used to detect entry of siRNA into cells. In siRNA functionality experiments, a siRNA of random sequence was used as a negative control to test for sequence-specific effects (siRandom). This siRNA was siCONTROL Non-Targeting siRNA #2 and was designed and screened by Dharmacon to have no silencing effect on any human, mouse or rat genes.

2.3. Primary cell cultures

Blood samples were obtained from healthy anonymous donors from the transfusion centers of Albacete and Madrid, following national guidelines. Peripheral blood mononuclear cells (PBMC) were isolated on a Ficoll-Hypaque density gradient (Rafer, Spain) following the current procedures of the Spanish HIV HGM BioBank [61]. PBMC were activated with the mitogen phytohemagglutinin (PHA) (2 μg/ml) and maintained in RPMI 1640 complete growth medium supplemented with 10% FBS and antibiotics along with interleukin-2 (20 U/ml).

2.4. Dendriplex formation

Dendriplexes were formed by mixing equal volumes of dendrimer and siRNA dissolved in OPTIMEM® I free of serum or antibiotics at concentrations depending on the +/− charge ratio and molar concentration desired [41,60]. The complexes were formed

at the following siRNA:dendrimer −/+ molar ratios: 1:1, 1:2, 1:4, 1:8, 1:12 and 1:16.

2.5. Computational details

3D atomistic models of dendrimer structures (**1-6**) were created using Materials Studio software package from Accelrys Inc. The RESP technique [62] was used for calculation of partial charges. For this charge parameterization the R.E.D.-III.5 tools [63] were used. The necessary QM calculations (QM structure minimizations, molecular electrostatic potential (MEP) calculations) were done using GAMESS [64]. The default, HF/6-31G*, level of theory was used for all charge-related QM calculations and the MEP potential was fitted on Connolly molecular surface. The GAFF (Generalized Amber Force Field) [65] force field was used for simulated dendrimers. Missing force field parameters were fitted by minimizing the differences between QM and force field based relative energies of properly chosen molecular fragments. 100 conformations of each molecular fragment were used for the force field parameters fitting. QM energies were calculated at MP2/HF/6-31G** level of theory using GAMESS and fitting was accomplished using *paramfit* routine from AMBER12 software [66]. Van der Waals parameters for Si atoms were taken from the MM3 force field. Computer model of siRNA (siNEF) molecule was created using NAB (Nucleic Acid Builder) module of AMBER12 software suite. This molecule was parameterized using Amber force field ff12SB [67]. First, the individual molecules were solvated in explicit water (TIP3P model) with the proper number Na^+ and Cl^- ions to preserve neutrality of the system and to ensure the correct ionic strength (0.15 M) [68]. These stand-alone systems were minimized (5000 steps with 5 kcal/(mol Å^2) restraint + 5000 without restraint), heated (200 ps of MD simulation, NVT, 5 kcal/(mol Å^2) restraint) to 310 K and equilibrated for 50 ns using Molecular Dynamics simulation (NPT ensemble, the first 0.5 ns with restrained solute, 2 kcal/(mol Å^2) restraint, T = 310 K and P = 0.1 MPa). These equilibrated molecular components were used to build the initial configurations of siRNA/dendrimer systems (one siNEF and four dendrimers in each system) using UCSF Chimera software, which was also used for final visualizations [69]. The same steps as in the case of individual components were done with complexes but the length of the simulation was now 115 ns (T = 310 K and P = 0.1 MPa). Hydrogens were constrained with the SHAKE algorithm to allow 2 fs time step [70] and Langevin thermostat with collision frequency 2 ps^{-1} was used for all MD runs [71]. The pressure relaxation time for weak-coupling barostat was 2 ps. Particle mesh Ewald method (PME) was used to treat long range electrostatic interactions under periodic conditions with a direct space cutoff of 10 Å. The same cutoff was used for van der Waals interactions. The *pmemd.cuda* module from Amber12 package was used for all the above described simulation steps [72]. For each dendrimer type, configurations obtained during the last 10 ns of the simulation were used for analysis of free energy of binding (with sampling step 0.1 ns i.e. 100 configurations were analyzed) using the molecular mechanics/Poisson–Boltzmann surface area (MM/PBSA) methodology supplemented by normal mode analysis. For this calculation set of modules (sander.APBS, NAB, etc.) interfaced through MMPBSA.py script was used [73]. Molecular mechanics calculations (MM) as well as the PBSA calculations were done using Amber12 module sander.APBS which uses Adaptive Poisson-Boltzmann Solver to calculate solvation energy contribution EPB [74]. The probe radius used for calculation of solvent accessible surface area (SASA) was 1.4 A. Default APBS value a = 0.02508 kcal*mol^{-1}*Å^{-2} of a parameter (surface tension) for calculation of the non-polar solvent contribution ENP = a*SASA was used. The dielectric constant of the solute was set to one and in the case of solvent to 80. Change in conformational entropy of the solute upon binding was estimated using normal mode analysis as implemented in NAB module taking implicitly in account also the solvation effects of salt water (i.e. nmode_igb = 1, nmode_istrng = 0.15). In case of these entropy calculations just 6 configurations (from the last 10 ns of simulation) were analysed due to the high time requirements. Single trajectory approach was used in this study.

3. Results and discussion

3.1. Synthesis of dendrimers

As commented in the introduction, shortening of reaction time is especially important in dendrimer synthesis. The preparation of dendrimers $[G_nO_3(NMe_3)_m]^{m+}$ (**1-3**, Figs. 1 and S1) and $[G_nO_3(NMe_2((CH_2)_2OH)_m]^{m+}$ (**4-6**, Figs. 1 and S2) have been reported elsewhere, two steps of this procedure being clearly longer than the others (scheme S1). With the aim to reduce reaction time, we have explored the use of microwaves in these two steps of the synthesis, since this technique is characterized by dramatically speeding up reactions.

One of them consists in the introduction of dendrons with peripheral vinyl functions to the polyphenoxo core, which requires heating at 90 °C for 60 h, and 6 and 21 days for the first, second, and third generation dendrimers, respectively. The use of microwaves in this reaction for first generation derivative was able to reduce the time to 150 min, after heating at 100 °C, obtaining the corresponding vinyl dendrimer $[G_1O_3V_m]$ in high yield. This procedure was not useful for higher generations, not observing reaction evolution in the conditions tested. However, these higher generation dendrimers can be obtained alternatively by hydrosilylation and alkenylation from lower generation precursors [75].

The second one is the formation of cationic compounds $[G_nO_3(NMe_2((CH_2)_2OH)_m]^{m+}$ (**4-6**) from neutral amine derivatives $[G_nO_3(NMe_3)_m]$, which are achieved by heating with $I(CH_2)_2OH$ at 60 °C for 3 days. Heating $I(CH_2)_2OH$ at higher temperatures led to its decomposition during the time that was required for this process. The use of microwave for this reaction reduced reaction time to 90 min heating at 100 °C, without observing decomposition of $I(CH_2)_2OH$, leading to $[G_nO_3(NMe_2((CH_2)_2OH)_m]^{m+}$ also in high yields. However, this procedure was only successful for small amounts of compounds (*ca.* 150 mg).

3.2. Biomedical assays

Peripheral blood mononuclear cells (PBMC) consist of lymphocytes (T cells, B cells, NK cells) and monocytes. HIV-1 use CD4 receptors to gain entry into host T-cells. These receptors are a protein found primarily on the surface of CD4T cells. To enter host cells, HIV-1 binds to a CD4 receptor and a coreceptor, either CCR5 or CXCR4, on the host cells, using for example the Nef protein. We are interested in the ability of siRNA Nef, which is the antisense sequence that codifies HIV Nef protein, to avoid HIV infection and for that reason we have studied the cationic dendrimers**1-6** as gene carriers for this siRNA.

First of all, we studied the toxicity of dendrimers $[G_nO_3(NMe_3)_m]^{m+}$ (**1-3**) and $[G_nO_3(NMe_2((CH_2)_2OH)_m]^{m+}$ (**4-6**) in PBMC by MTT assays to measure mitochondrial metabolic activity. The data showed an increase of toxicity from first to second generation dendrimer, whilst close values were found for second and third generation dendrimers (Fig. 2). Regarding type of ammonium function, no significant differences were observed for both types of cationic dendrimers.

Formation of dendriplexes between dendrimers and siRNA Nef were analyzed by Z potential (Fig. S3). The curve shapes were very similar for dendrimer of same generations but in case of second

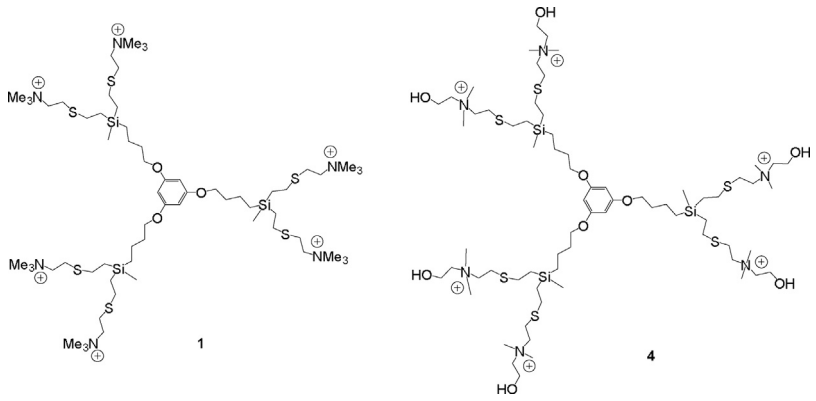

Fig. 1. Drawing of first generation cationic dendrimers **1** and **4**.

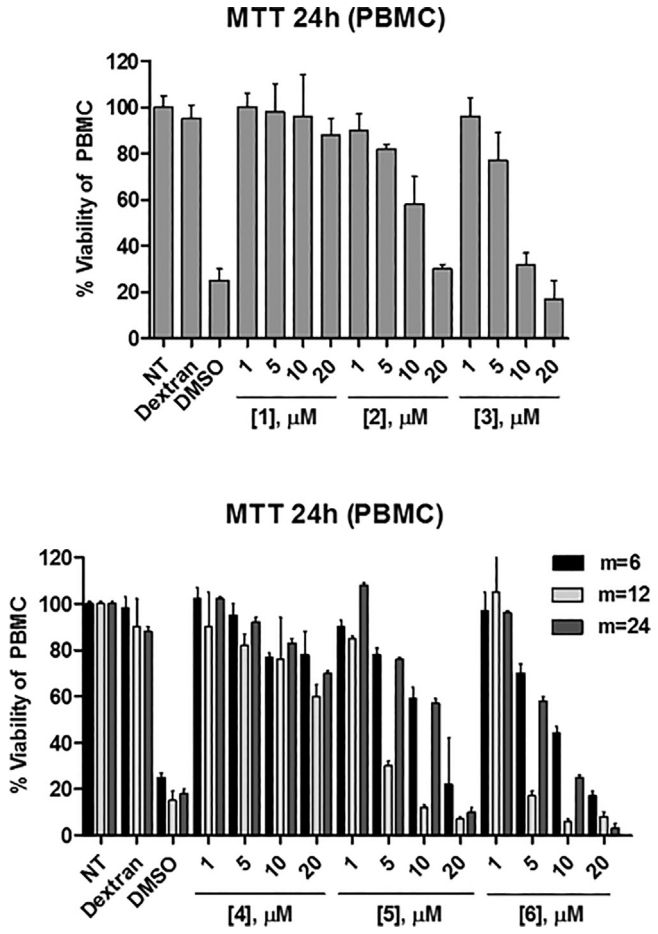

Fig. 2. Toxicity (MTT) of $[G_nO_3(NMe_3)_m]^{m+}$ (**1-3**) and $[G_nO_3(NMe_2((CH_2)_2OH)_m]^{m+}$ (**4-6**) (n = 1, m = 6; n = 2, m = 12; n = 3, m = 24) in PBMC after 24 h of treatment with the different nanosystems at various concentrations. Data are presented as percent of living cells compared with control cells as 100% of viable cells (mean ± SD of three individual experiments).

generation derivatives. Particularly for **2**, it was necessary highest +/− charge ratio for stabilization of dendriplexes.

Electrophoresis analyses in agarose gel were also performed to study the binding capacity of dendrimers **1-6** toward siRNA Nef. For the first family of compounds, $[G_nO_3(NMe_3)_m]^{m+}$ (**1-3**) (Fig. 3), the usual generation dependent behaviour was observed: the dendriplex stability increases with dendrimer charge. [58] At adequate ratios, the dendriplex is formed after 2 h, being the siRNA released after 24 h. These ratios are below dendriplexes toxicity (Figs. S4 and S5), meaning potential applicability as carriers. For the second family of dendrimers, surprisingly, the lowest ratio RNA/dendrimer for stabilizing dendriplexes was for first generation derivative **4**, whereas the other two dendrimers follow the expected order (Fig. 4). Dendriplex formation for **4** was observed at −/+ molar ratio 1/4, whereas a −/+ molar ratio of 1/12 was necessary for formation of dendriplex with **1**. On the other hand, stable dendriplexes for second generation dendrimers were achieved at lower ratio for **2** than for **5**, whist dendriplexes for third generation dendrimers (**3**, **6**) were obtained at similar ratios. In the case of **5**, dendriplex stabilization was produced over biocompatible concentration (Fig. S5) and was discarded for next experiments. The abnormal stability of the dendriplex formed with first generation dendrimer **4** (with $-(NMe_2((CH_2)_2OH))^+$ functions) points out to an important influence of the hydroxyl groups in this compound **4**. Dendrimer **1** and **4** are smaller and internalize into siRNA strands (see Section 3.3). Additionally, the hydroxyl groups stablish hydrogen bridges with siRNA to reinforce the interaction. This situation differs for the higher generation derivatives of theses series, which stability depends mainly on electrostatic interaction (see above and molecular modelling section). In the case of **5**, the ammonium groups $-(NMe_2((CH_2)_2OH))^+$ seems to hamper dendriplex formation in comparison with the analogue dendrimer with $-NMe_3^+$ groups (**2**). For third generation dendrimers, **3** and **6**, the type of ammonium function apparently does not affect the dendriplex formation.

The dendriplexes stability was evaluated by heparin competition assays in the absence and in the presence of RNase (Fig. 5). Heparin is a polysulfated glycosaminoglycan that competes with nucleic acids in their interaction with cationic dendrimers due to its anionic charge. This experiment was performed to simulate *in vivo* conditions, since interaction of dendriplexes with a diversity of proteins or nucleic acids can weaken the system favouring the release of the RNA. The −/+ molar ratio of dendriplexes that has been used for this experiment corresponds with the best results found in the biocompatibility assays (1:12 for **1** and **2**, 1:8 for **3**, 1:4 for **4**, and 1:2 for **6**). The formation of heparin/dendriplex complexes was spontaneous after mixing heparin and the cationic dendrimer in aqueous solution, probably via electrostatic interactions. Polyacrylamide gel electrophoresis (PAGE) was used to adequately visualize the siRNA released from the dendriplex. Of all the compounds analyzed, only dendriplex obtained with dendrimer **3** is sufficiently stable to protect RNA from degradation. Hence, dendrimers with cationic groups of the type $[-NMe_2(CH_2)_2OH]^+$ do not interact strong enough with siNef under compatible concentrations (see molecular modelling section).

In view of the previous data, only the dendriplex formed with $[G_3O_3(NMe_3)_{24}]^{24+}$ (**3**) was selected for an inhibition test in PBMC

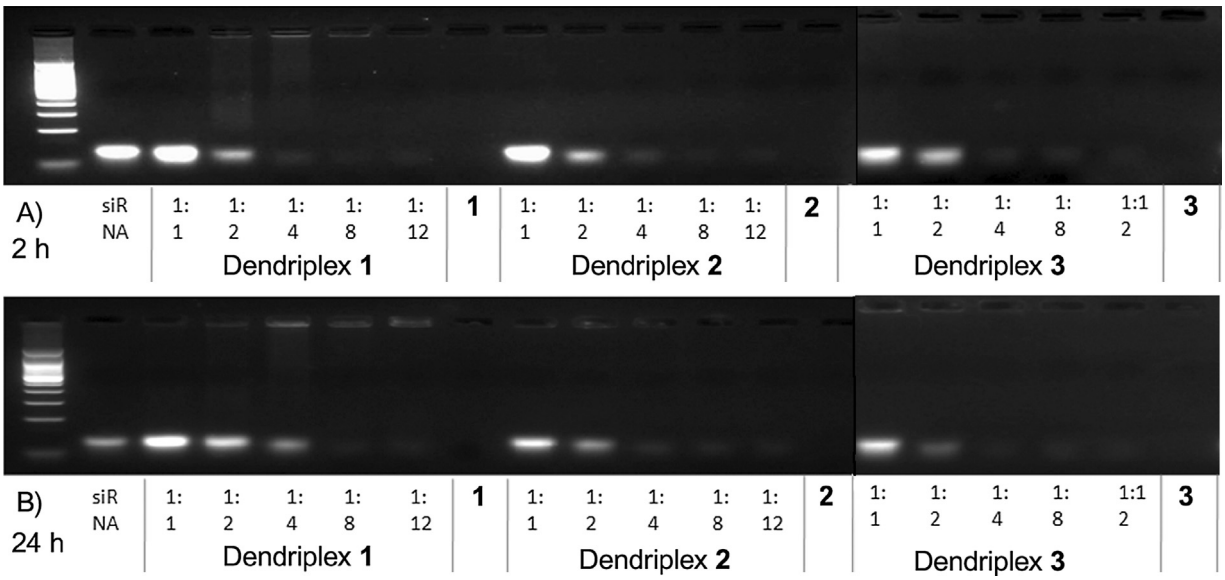

Fig. 3. Electrophoresis gel in agarose of dendriplexes formed with dendrimers $[G_nO_3(NMe_3)_m]^{m+}$ (**1-3**) at different siRNA Nef:dendrimer −/+ molar ratios after 2 h (3A) and 24 h (3B).

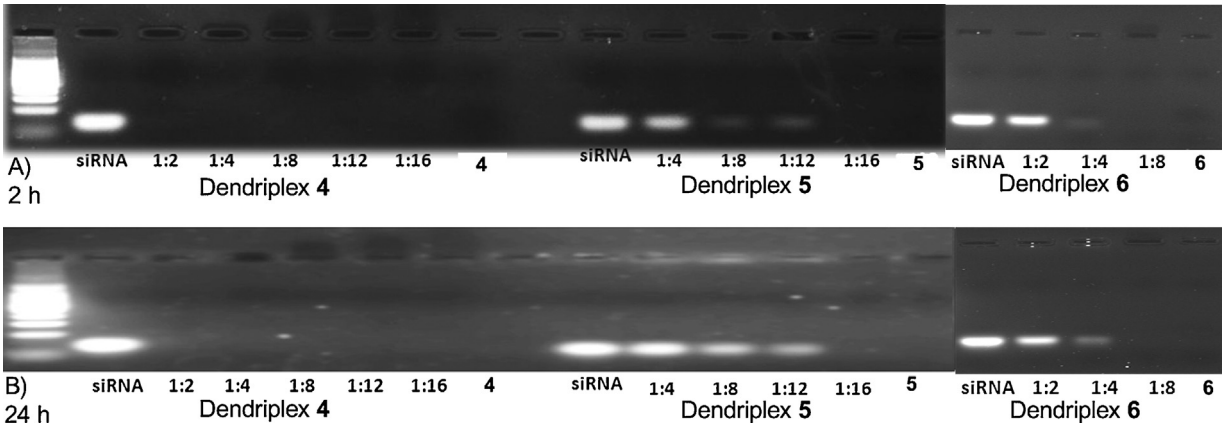

Fig. 4. Electrophoresis gel in agarose of dendriplexes formed with dendrimers $[G_nO_3(NMe_2((CH_2)_2OH)_m]^{m+}$ (**4-6**) at different siRNA Nef:dendrimer −/+ molar ratios after 2 h (4A) and 24 h (4B).

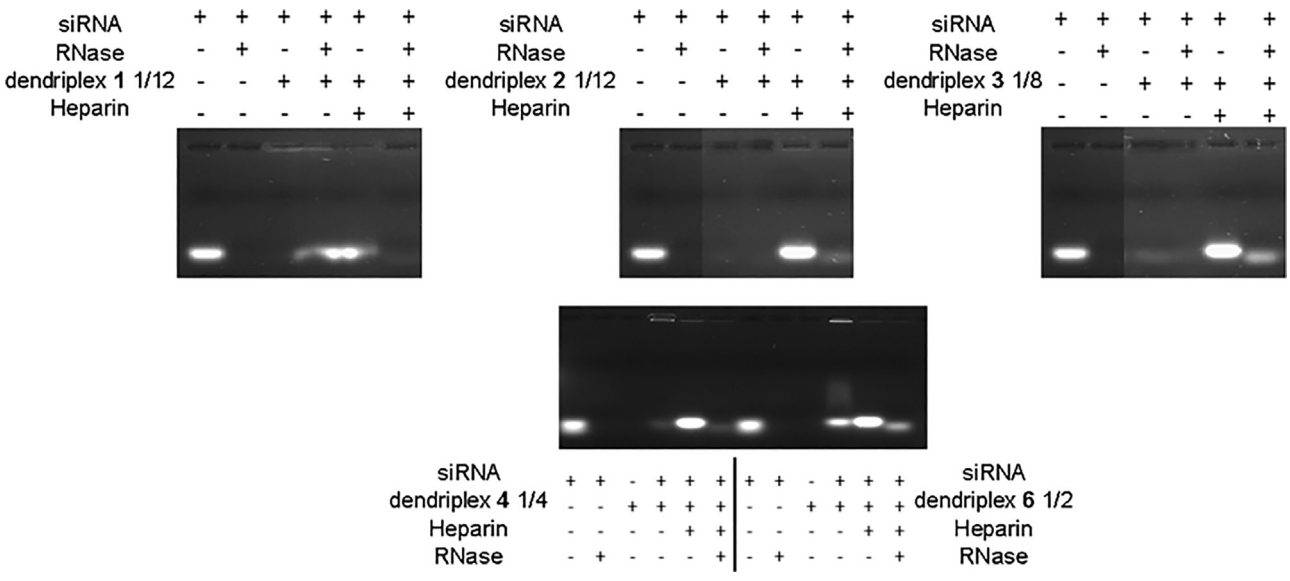

Fig. 5. Polyacrylamide gel electrophoresis of dendriplexes/heparine competition and RNase degradation assays after 24 h.

(Fig. S6). The result of this experiment showed that dendriplex **3**/siRNA Nef at molar ratio 1/8 (−/+) produced low infection inhibition (Fig. S7), probably due to low transfection efficacy or to the inability of dendrimer **3** to properly release the siRNA.

3.3. Molecular modelling

The computer modeling was used to obtain detail information about the interactions of cationic dendrimers $[G_nO_3(NMe_2R)_m]^{m+}$ (R = Me (**1-3**), $(CH_2)_2OH$) (**4-6**) with siNEF in salt water (IS = 0.15) under the given thermodynamic conditions (T = 310 K, P = 1 bar). The influence of dendrimer surface groups as well as generation on their ability to bind siNEF was investigated. To mimic one of the usual experimental molecular ratio siNEF/dendrimers = 1/4, the main components of simulated systems were one siNEF molecule and four dendrimers of the given type. These solvated systems were simulated using Molecular Dynamics (NPT ensemble) for 115 ns. In all 6 cases, simulations showed ability of dendrimers to create stable complex with siNEF (Figs. 6 and S8). Let's notice here that in case of third generation dendrimers (**3** and **6**) the complexes in the given molecular ratio (1/4) are stable just thanks to the salt water environment and in vacuum they can't exist. This is evident from their high positive values of binding enthalpies in vacuum ΔH_gas (Table S1). This is due to the fact that the third generation dendrimers **3** and **6** have net charge +24 and so the net charge of four such dendrimers is +96 while the net charge of the siNEF molecule is −38.

In case of the first generation dendrimers **1** and **4**, simulations revealed ability of these small flexible molecules to partly penetrate into the siRNA structure at the ends of siRNA strands (Figs. 6 and S8 and S10). In this disposition the charged end groups and eventually polar hydroxyl groups (in case of **4**, Fig. 6) are used for the electrostatic or H-bond interactions with negatively charged siRNA backbone, some nucleotides or surrounding water molecules. Dendrimer **4** shows moreover higher stability in such wedged positions than dendrimer **1** due to formation of hydrogen bonds (8 H-bonds in the final conformation) between its hydroxyl groups, which are not present in dendrimer **1**, and the siNEF. Some added value of H-bond interactions in case of dendrimer **4**, compared to dendrimer **1**, is apparent also in other binding sites (Table S1). In both cases, dendrimers **1** and **4**, there is evident tendency for the specific "stacking" interaction between the dendrimer core polyphenol unit and terminal uracil nucleobase of each siRNA strand (Figs. 6 and S8–S10). This interaction is not possible for higher dendrimers because the polyphenoxo core is inaccessible due to the increasing size of the branches around it.

For each dendrimer we estimated the free energy of binding $\Delta G = \Delta H - T\Delta S$ (ΔH, ΔS are the enthalpy and entropy change due to the binding) with respect to the rest of the complex (siNEF + 3 remaining dendrimers) using MM/PBSA and normal mode analysis approaches. The minimal ΔG values ΔG_min (the highest affinity) as well as the average values ΔG_average (averages over all four dendrimers belonging to the same complex) are reported in Fig. S11. Free binding energies as well as all the energetic contributions for each individual dendrimer molecule are reported in table S1. As can be deduced, the affinity increases with growing generation but for first generation dendrimer **4** (compare ΔG_average values). If we compare the energies corresponding to the strongest bound dendrimer in each dendriplex, the above mentioned trend is violated in case of OH-terminated dendrimers by the first generation dendrimer **4** (compare ΔG_min values). We can also notice that except the first generation dendrimers (**1**, **4**) the −OH terminated molecules have slightly worse affinity than the same generation dendrimers whose branches are terminated with–NMe_3^+ ammonium groups. The highest affinity (the lowest value of ΔG = −102.85 kcal/mol) in case of dendriplex formed with dendrimers **4** belongs to the dendrimer molecule that is the best incorporated into the siRNA structure (Figs. 6, S8–S11 and Table S1). As can be seen in Fig. S11 and Table S1, the estimated ΔG value in case of this wedged dendrimer **4** molecule is the second best between all 6×4 complexed dendrimer molecules. The ability of dendrimer **4** to find stable position partly inside the siRNA structure might be connected with the experimental fact that with this dendrimer the smallest +/− ratio was used to form a stable dendriplex. Along with the relatively high binding energy, we should also consider the fact that such "hidden" dendrimers are also less accessible to the surrounding molecules that could participate on "unbinding" processes inside the cell. Even if some siRNA is liberated from the main dendriplex (composed of tens or hundreds of siRNA and dendrimer molecules) but still with such wedged dendrimer/s incorporated in its structure, the final processing (i.e. division into two single strands) might be problematic.

The different types of interactions between dendrimers and siRNA and the energy of these interactions justify also the results observed in the heparin competition assays. Taking into account that heparin is a polyanionic molecule, the stability difference of dendrimer/heparin and dendrimer/siRNA complexes is the key point for the final result. Molecular modelling is done to evaluate the particular stability of each dendrimer with siRNA Nef. The most stable dendriplex is that composed of siRNA and dendrimer **3** (Fig. S11 or Table S1), which is in good agreement with the results obtained from heparin competition assays. This is the bigger dendrimer and its interaction with RNA is pure electrostatic. Due to its size and charge, its displacement from the RNA surface is more difficult, so the interaction of the phosphate groups with the RNase is hampered. Also, the fact that the dendrimer **4** did not succeeded in heparin competition test is rather consistent with the simulation results. The stabilization of this dendriplex is done by electrostatic interaction and by hydrogen bond formation of one dendrimer internalized into the RNA strand. The dendrimers on the RNA surfaces, those interacting electrostatically, are displaced by heparin and subsequently the phosphate groups are accessible to the RNase. The dendrimer located into the RNA, even if it not displaced by heparin, would not affect this process since in this disposition it does not block any phosphate groups.

3.4. Single molecule force spectroscopy assays

In order to test if dendrimers bind to siRNA we have carried out single molecule pulling experiments using optical tweezers [76]. We have focused our studies on first generation dendrimers **1** and **4**. As substrate, we have used an RNA hairpin model system suitable for the mechanical pulling assays which unfolding and folding kinetics has been extensively studied by some of us [77]. The RNA contains a stem of 20 bps ending in a tetraloop (GAAA) (Fig. 7a), which is inserted between molecular RNA/DNA hybrid handles of 527 bps and 599 bps flanking at both sides (Fig. 7a). In the optical tweezers setup, two counter-propagating laser beams that are focused using two high numerical aperture (1.2) objectives in a microfluidics chamber produce the optical trap. Force is directly measured by detecting the change in light momentum using photosensitive detectors [78]. The molecular construct (RNA hairpin plus handles) is tagged at one end with a single biotin and multiple digoxigenins at the other end. The construct is then tethered between two micron-sized beads, one is coated with streptavidin whereas the other is coated with anti-dig [78]. Connections to beads are made through distinct biotin-streptavidin and antigen-antibody bonds. One bead is captured in the optical trap and used to measure the force by collecting the deflected light, the other is immobilized in the tip of a glass micropipette by air suction. The RNA molecules were introduced in a microfluidics chamber in a 1 M TRIS-HCl (pH 7.5) buffer solution containing 30 nM dendrimers. The

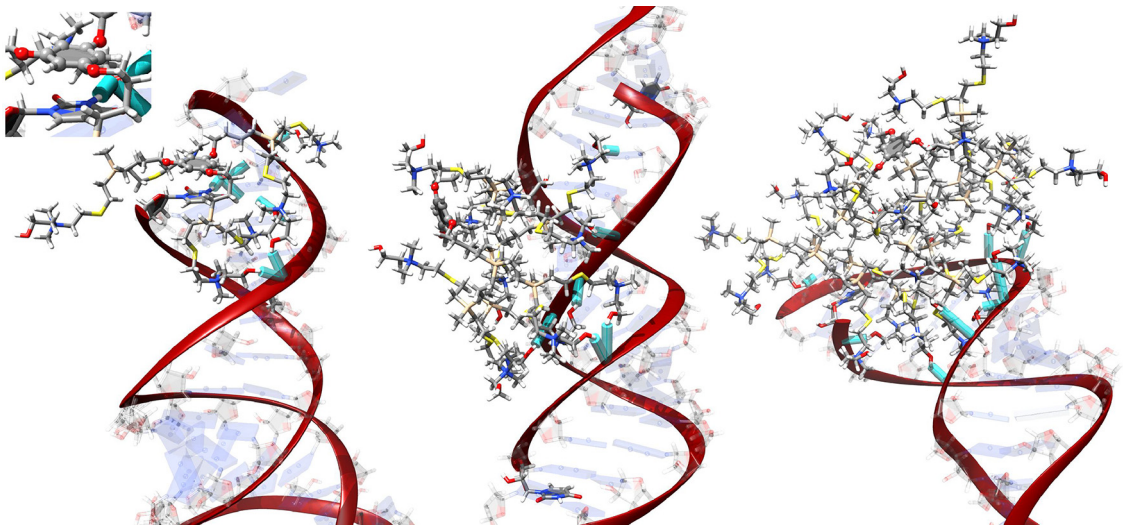

Fig. 6. Visualization of dendrimers $[G_nO_3(NMe_2((CH_2)_2OH)_m]^{m+}$ (**4-6**) (from left to the right) bound to siNEF. From each of the four dendrimers belonging to a given dendriplex just that with highest affinity estimate (i.e. corresponding to ΔG_min values in Fig. S11) is shown for better clarity. In the top-left corner there is shown detail of interaction between the core ring of dendrimer **4** and the terminal uracil nucleobase. The color coding for atoms is: C, grey; H, white; O, red; Si, beige; S, yellow. Cyan cylinders denote actual hydrogen bonds between dendrimer and siNEF. The core dendrimer polyphenol ring is filled and atoms are in ball representation. Also nucleobase ring of the terminal uracil is filled. The other nucleotides are shown just schematically and are almost transparent for better clarity.

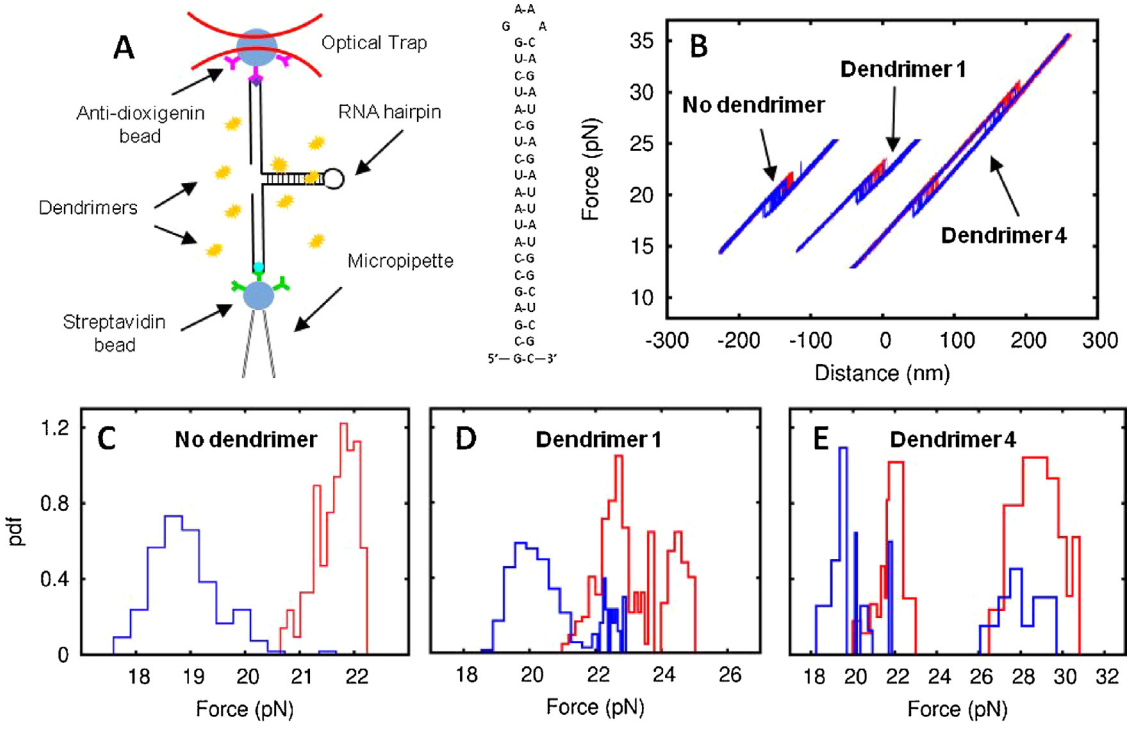

Fig. 7. Single molecule experimental setup and results. (A) Experimental setup and RNA sequence. (B) Pulling cycles for the RNA hairpin without dendrimer (left), in the presence of dendrimer **1** (middle) and dendrimer **4** (right). Unfolding (red) and folding (blue) trajectories for each case. (C-E) Experimental distributions for the first rupture force (red) and the first refolding force (blue) for the RNA hairpin without dendrimer, and in the presence of dendrimer **1** and **4**, respectively. (For interpretation of the references to colour in this figure legend, the reader is referred to the web version of this article.)

interaction between dendrimers **1** and **4** with the RNA hairpin was investigated by moving the optical trap relative to the pipette using piezo actuators at a speed of 100 nm/s. Fig. 7b shows various pulling cycles for the RNA (without dendrimer, left), and in the presence of dendrimer **1** (middle) and dendrimer **4** (right). Hysteresis effects between the unfolding (red) and refolding (blue) forces are generally observed indicating that mechanical unfolding and folding is carried out under irreversible conditions. We have measured the unfolding and folding force distributions and the results are shown in Fig. 7c–e for the three cases. In the absence of dendrimers the RNA unfolds at a force of about 20 pN reflecting the mechanical stability of the folded native structure of the hairpin. Interestingly, in the presence of dendrimers a fraction of all rupture force events are observed at higher forces, about 23 pN for dendrimer **1** and 29 pN for dendrimer **4**, reflecting that dendrimers have bound to the RNA thereby increasing their mechanical stability to unfolding. These experiments demonstrate the higher kinetic stability of dendrimer **4** binding to RNA as compared to dendrimer **1**, in agreement

with the above mentioned results from electrophoretic bulk assays and molecular dynamics simulations. The higher kinetic stability observed for dendrimer **4** also implies a higher binding affinity in equilibrium, which might be estimated by conducting additional experiments combined with mathematical methods [79].

4. Conclusions

The study of dendriplexes formation between dendrimers of the type $[G_nO_3(NMe_3)_m]^{m+}$ (**1-3**) and $[G_nO_3(NMe_2((CH_2)_2OH)_m]^{m+}$ (**4-6**), with different ammonium peripheral groups, and siRNA Nef reveals that the type and strength of interaction depend on generation and type of ammonium groups. In general, higher generation and cationic $[\text{-}NMe_3]^+$ groups favour more stable dendriplexes as consequence of larger cationic charges and higher charge exposure, respectively. In case of the second and third generations, the dendrimer/siRNA binding is based mainly on electrostatic and van der Waals interactions between the dendrimer surface groups and siRNA, whereas the first generation dendrimers are also able to internalize into siRNA Nef structure establishing π-stacking interactions between the polyphenoxo core and terminal uracil nucleobase of siRNA strands. This last interaction is clearly weaker than the other two. However, dendrimer $[G_1O_3(NMe_2((CH_2)_2OH)_6]^{6+}$ (**4**) achieved considerable stabilization of this inner disposition due to the combination of above mentioned π-stacking interactions and H-bond interactions between —OH groups of dendrimers and negatively charged siRNA backbone of some nucleotides. These results were validated with single molecule force assays, which showed that first-generation dendrimers **1** and **4** bind to RNA with different strengths

The applicability of these dendriplexes as siRNA carriers is determined not only by the stability of dendriplexes but also by their ability to protect siRNA from degradation. Therefore, and within compatibility range, only compound $[G_3O_3(NMe_3)_{24}]^{24+}$ (**3**) fulfils these requirements. This dendriplex is the one with high stabilization energy, as was confirmed by molecular modelling. In the particular case of dendriplex formed with $[G_1O_3(NMe_2((CH_2)_2OH)_6]^{6+}$ (**4**), the small size of dendrimer together with its intraRNA disposition do not avoid interaction with RNases and siRNA degradation is produced.

Therefore, structural manipulation of cationic dendrimers can lead to a variety of interaction situations with nucleic acids that could be used to modulate the affinity between both systems and thus, find an adequate carrier for nucleic acids.

Acknowledgments

This work has been supported by grants from CTQ-2014-54004-P (MINECO) to R.G. This work has been (partially) funded by the RD12/0017/0037 and RD16/0025/0019, projects as part of Acción Estratégica en Salud, Plan Nacional de Investigación Científica, Desarrollo e Innovación Tecnológica (2008–2011, 2013–2016) and cofinanced by Instituto de Salud Carlos III (Subdirección General de Evaluación) and Fondo Europeo de Desarrollo Regional (FEDER), RETIC PT13/0010/0028, Fondo de Investigacion Sanitaria (FIS) (grant number PI16/01863, PI14/00882) and CYTED 214RT0482 (M.A.M.-F.). We particularly acknowledge the Spanish HIV HGM BioBank integrated in the Spanish AIDS Research Network and the National Network BioBank and supported by the Instituto Salud Carlos III. F.R. acknowledges support from ICREA Academia 2013 and Spanish Research Council Grant FIS2016-80458-P. CIBER-BBN is an initiative funded by the VI National R&D&i Plan 2008–2011, Iniciativa Ingenio 2010, the Consolider Program, and CIBER Actions and financed by the Instituto de Salud Carlos III with assistance from the European Regional Development Fund (R.G: and M.A M.-F.). This work was co-financed by the Czech Science Foundation (project No. 15-05903S) and the Research Infrastructure NanoEnviCz, supported by the Ministry of Education, Youth and Sports of the Czech Republic under project No. LM2015073. UCSF Chimera development is supported by NIGMS P41-GM103311. M.S.M. acknowledges UAH for a fellowship.

Appendix A. Supplementary data

Supplementary data associated with this article can be found, in the online version, at https://doi.org/10.1016/j.colsurfb.2017.12.009.

References

[1] I.M. Verma, N. Somia, Nature 389 (1997) 239–242.
[2] E. Wagner, Mol. Ther. 16 (2008) 1–2.
[3] M. Cavazzana-Calvo, A. Fischer, J. Clin. Investig. 117 (2007) 1456–1465.
[4] C.R. Dass, J. Pharm. Pharmacol. 54 (2002) 3–27.
[5] K. Kodama, Y. Katayama, Y. Shoji, H. Nakashima, Curr. Med. Chem. 13 (2006) 2155–2161.
[6] Z. Sideratou, L.A. Tziveleka, C. Kontoyianni, D. Tsiourvas, C.M. Paleos, Gene Ther. Mol. Biol. 10A (2006) 71–94.
[7] G.A. Pietersz, C.K. Tang, V. Apostolopoulos, Mini-Rev. Med. Chem. 6 (2006) 1285–1298.
[8] M. Elfinger, S. Uezguen, C. Rudolph, Curr. Nanosci. 4 (2008) 322–353.
[9] E. Fattal, A. Bochota, Int J. Pharm. 364 (2008) 237–248.
[10] M.A. Mintzer, E.E. Simanek, Chem. Rev. 109 (2009) 259–302.
[11] X. Guo, L. Huang, Acc. Chem. Res. 45 (2012) 971–979.
[12] J.-P. Behr, Acc. Chem. Res. 45 (2012) 980–984.
[13] R.G. Denkewalter, J.F. Kolc, W.J. Lukasavage, US Pat 4, 410, 688, 1983.
[14] F. Vögtle, C.A. Schalley, Top. Curr. Chem. (2003) 228.
[15] G.R. Newkome, C.N. Moorefield, F. Vögtle, Dendrimers and Dendrons: Concepts, Syntheses Applications, Wiley-VCH, Weinheim, Germany, 2001.
[16] G.R. Newkome, C.D. Shreiner, Polymer 49 (2008) 1–173.
[17] D.A. Tomalia, J.M.J. Fréchet, J. Polym. Sci. Part A: Pol. Chem. 40 (2002) 2719–2728.
[18] J.M.J. Fréchet, D.A. Tomalia, Dendrimers and Other Dendritic Polymers VCH, 2002, Weinheim.
[19] D. Astruc, E. Boisselier, C. Ornelas, Chem. Rev. 110 (2010) 1857–1959.
[20] X. Liu, P. Rocchi, L. Peng, New J. Chem. 9 (2012) 256–263.
[21] P.M.H. Heegaard, U. Boas, N.S. Sorensen, Bioconjugate Chem. 21 (2010) 405–418.
[22] D.G. Shcharbin, B. Klajnert, M. Bryszewska, Biochemistry 74 (2009) 1070–1079.
[23] H. Zhong, Z.G. He, Z. Li, G.Y. Li, S.R. Shen, X.L. Li, J. Biomater. Appl. 22 (2008) 527–544.
[24] D.K. Smith, Curr. Top. Med. Chem. 8 (2008) 1187–1203.
[25] Y. Gao, G. Gao, Y. He, T.L. Liu, R. Qi, Mini-Rev. Med. Chem. 8 (2008) 889–900.
[26] H.S. Parekh, Curr. Pharm. Des. 13 (2007) 2837–2850.
[27] M. Guillot-Nieckowski, S. Eisler, F. Diederich, New J. Chem. 31 (2007) 1111–1127.
[28] C. Dùfes, I.F. Uchegbu, A.G. Schatzlein, Adv. Drug Deliv. Rev. 57 (2005) 2177–2202.
[29] K.L. Wooley, C.J. Hawker, J.M.J. Fréchet, Angew. Chem. Int. Ed. Engl. 33 (1994) 82–85.
[30] F. Zeng, S.C. Zimmerman, J. Am. Chem. Soc. 118 (1996) 5326–5327.
[31] L. Brauge, G. Magro, A. Caminade, J. Majoral, J. Am. Chem. Soc. 123 (2001) 6698–6699.
[32] P. Antoni, M.J. Robb, L. Campos, M. Montanez, A. Hult, E. Malmström, M. Malkoch, C.J. Hawker, Macromolecules 43 (2010) 6625–6631.
[33] P. Dvornic, M.J. Owen and Eds, Springer: Berlin, 2009.
[34] E. Fuentes-Paniagua, J.M. Hernández-Ros, M. Sánchez-Milla, M.A. Camero, M. Maly, J. Pérez-Serrano, J.L. Copa-Patiño, J. Sánchez-Nieves, J. Soliveri, R. Gómez, F.J. de la Mata, RSC Adv. 4 (2014) 1256–1265.
[35] E. Fuentes-Paniagua, J. Sánchez-Nieves, J.M. Hernández-Ros, A. Fernández-Ezequiel, J. Soliveri, J.L. Copa-Patiño, R. Gómez, F.J. de la Mata, RSC Adv. 6 (2016) 7022–7033.
[36] M.J. Serramía, S. Álvarez, E. Fuentes-Paniagua, M.I. Clemente, J. Sánchez-Nieves, R. Gómez, F.J. de la Mata, M.A. Muñoz-Fernández, J. Control. Release 200 (2015) 60–70.
[37] J.L. Jiménez, M.I. Clemente, N.D. Weber, J. Sánchez, P. Ortega, F.J.d.l. Mata, R. Gómez, D. García, L.A. López-Fernández, M.A. Muñoz-Fernández, BioDrugs 24 (2010) 331–343.
[38] E. Fuentes-Paniagua, M.J. Serramía, J. Sánchez-Nieves, S. Álvarez, M.A. Muñoz-Fernández, R. Gómez, F.J. de la Mata, Eur. Polym. J. 71 (2015) 61–72.
[39] T. Gonzalo, M.I. Clemente, L. Chonco, N.D. Weber, L. Díaz, M.J. Serramía, R. Gras, P. Ortega, F.J. de la Mata, R. Gómez, L.A. López-Fernández, M.A. Muñoz-Fernández, J.L. Jiménez, Chem. Med. Chem. 5 (2010) 921–929.

[40] I. Posadas, B. López-Hernández, M.I. Clemente, J.L. Jiménez, P. Ortega, F.J. de la Mata, R. Gómez, M.A. Muñoz-Fernández, V. Ceña, Pharm. Res. 26 (2009) 1181–1191.
[41] N. Weber, P. Ortega, M.I. Clemente, D. Shcharbin, M. Bryszewska, F.J. de la Mata, R. Gómez, M.A. Muñoz-Fernández, J. Control Release 132 (2008) 55–64.
[42] J.F. Bermejo, P. Ortega, L. Chonco, R. Eritja, R. Samaniego, M. Mullner, E. de Jesús, F.J. de la Mata, J.C. Flores, R. Gómez, A. Muñoz-Fernández, J. Chem. Eur. 13 (2007) 483–495.
[43] P. Ortega, J.F. Bermejo, L. Chonco, E. de Jesús, F.J. de la Mata, G. Fernández, J.C. Flores, R. Gómez, M.J. Serramía, M.A. Muñoz-Fernández, Eur. J. Inorg. Chem. (2006) 1388–1396.
[44] M. Ionov, Z. Garaiova, I. Waczulikova, D. Wrobel, E. Pedziwiatr-Werbicka, R. Gómez-Ramírez, F.J. de la Mata, B. Klajnert, T. Hianik, M. Bryszewska, Biochim. Biophys. Acta-Biomembr. 1818 (2012) 2209–2216.
[45] A.J. Perisé-Barrios, J.L. Jiménez, A. Domínguez-Soto, F.J. de la Mata, A.L. Corbí, R. Gómez, M.A. Muñoz-Fernández, J. Control Release 184 (2014) 51–57.
[46] J. Sánchez-Nieves, P. Fransen, D. Pulido, R. Lorente, M.A. Muñoz-Fernández, F. Albericio, M. Royo, R. Gómez, E.J. de la Mata, Eur. J. Med. Chem. 76 (2014) 43–52.
[47] N. de las Cuevas, S. García-Gallego, B. Rasines, F.J. de la Mata, L.G. Guijarro, M.Á. Muñoz-Fernández, R. Gómez, Curr. Med. Chem. 19 (2012) 5052–5061.
[48] A.-M. Caminade, S. Fruchon, C.-O. Turrin, M. Poupot, A. Ouali, A. Maraval, M. Garzoni, M. Maly, V. Furer, V. Kovalenko, J.-P. Majoral, G.M. Pavan, R. Poupot, Nat. Commun. 6 (7722) (2015) 7711–7721.
[49] K. Hatano, T. Matsubara, Y. Muramatsu, M. Ezure, T. Koyama, K. Matsuoka, R. Kuriyama, H. Kori, T. Sato, J. Med. Chem. 57 (2014) 8332–8339.
[50] J. Haensler, F.C. Szoka, Bioconjugate Chem. 4 (1993) 372–379.
[51] J. Morales-Sanfrutos, A. Megía-Fernández, F. Hernández-Mateo, M.D. Girón-González, R. Salto-González, F. Santoyo-González, Org. Biomol. Chem. 9 (2011) 851–864.
[52] J.L. Santos, H. Oliveira, D. Pandita, J. Rodrigues, A.P. Pego, P.L. Granja, H. Tomas, J. Control. Release 144 (2010) 55–64.
[53] H. Liu, Y. Wang, M. Wang, J. Xiao, Y. Cheng, Biomaterials 35 (2014) 5407–5413.
[54] B. Nandy, M. Santosh, P.K. Maiti, J. Biosci. 37 (2012) 457–474.
[55] C. Sun, T. Tang, H. Uludağ, J. Phys. Chem. B 116 (2012) 2405–2413.
[56] C. Sun, T. Tang, H. Uludag, Biomacromolecules 12 (2011) 3698–3707.
[57] M. Zheng, G.M. Pavan, M. Neeb, A.K. Schaper, A. Danani, G. Klebe, O.M. Merkel, T. Kissel, ACS Nano 6 (2012) 9447–9454.
[58] G.M. Pavan, ChemMedChem 9 (2014) 2623–2631.
[59] A.T. Das, T.R. Brummelkamp, E.M. Westerhout, M. Vink, M. Madiredjo, R. Bernards, B. Berkhout, J. Virol. 78 (2004) 2601–2605.
[60] J.L. Jiménez, M.I. Clemente, N.D. Weber, J. Sánchez, P. Ortega, F.J. de la Mata, R. Gómez, D. García, L.A. López-Fernández, M.A. Muñoz-Fernández, BioDrugs 24 (2010) 331–343.
[61] I. García-Merino, N.d.L. Cuevas, J.L. Jiménez, J. Gallego, C. Gómez, C. Prieto, M.J. Serramía, R. Lorente, M.Á. Muñoz-Fernández, Retrovirology 6 (2009) 27.
[62] C.I. Bayly, P. Cieplak, W.D. Cornell, P.A. Kollman, J. Phys. Chem. 97 (1993) 10269.
[63] F.-Y. Dupradeau, A. Pigache, T. Zaffran, C. Savineau, R. Lelong, N. Grivel, D. Lelong, W. Rosanski, P. Cieplak, Phys. Chem. Chem. Phys. 12 (2010) 7821.
[64] M.W. Schmidt, K.K. Baldridge, J.A. Boatz, S.T. Elbert, M.S. Gordon, J.H. Jensen, S. Koseki, N. Matsunaga, K.A. Nguyen, S. Su, T.L. Windus, M. Dupuis, J.A. Montgomery, J. Comput. Chem. 14 (1993) 1347–1363.
[65] J. Wang, R.M. Wolf, J.W. Caldwell, P.A. Kollamn, D.A. Case, J. Comput Chem, (2004) 1157–1174.
[66] D.A. Case, T.A. Darden, T.E. Caaaaa, III, C.L. Simmerling, J. Wang, R.E. Duke, R. Luo, R.C. Walker, W. Zhang, K.M. Merz, B. Roberts, S. Hayik, A. Roitberg, G. Seabra, J. Swails, A.W. Goetz, I. Kolossváry, K.F. Wong, F. Paesani, J. Vanicek, R.M. Wolf, J. Liu, X. Wu, S.R. Brozell, T. Steinbrecher, H. Gohlke, Q. Cai, X. Ye, J. Wang, M.-J. Hsieh, G. Cui, D.R. Roe, D.H. Mathews, M.G. Seetin, R. Salomon-Ferrer, C. Sagui, V. Babin, T. Luchko, S. Gusarov, A. Kovalenko, P.A. Kollman, University of California, San Francisco, 2012, AMBER 12.
[67] J.-H. Lii, A. Norman, L. Allinger, J. Comput. Chem. 12 (1991) 186–199.
[68] W.L. Jorgensen, J. Chandrasekhar, J. Madura, M.L. Klein, J. Chem. Phys. 79 (1983) 926–935.
[69] Z. Yang, K. Lasker, D. Schneidman-Duhovny, B. Webb, C.C. Huang, E.F. Pettersen, T.D. Goddard, E.C. Meng, A. Sali, T.E. Ferrin, J. Struct. Biol. 179 (2012) 269.
[70] J.-P. Ryckaert, G. Ciccotti, H.J.C. Berendsen, J. Comput Phys, (1977) 327–341.
[71] X. Wu, B.R. Brooks, Chem. Phys. Lett. 381 (2003) 512–518.
[72] R. Salomon-Ferrer, A.W. Goetz, D. Poole, S. Le Grand, R.C. Walker, J. Chem. Theory Comput. 9 (2013) 3878.
[73] B.R. Miller III, T.D. McGee Jr., J.M. Swails, N. Homeyer, H. Gohlke, A.E. Roitberg, J. Chem. Theory Comput. 8 (2012) 3314–3321.
[74] N.A. Baker, D. Sept, S. Joseph, M.J. Holst, J.A. McCammon, Proc. Natl. Acad. Sci. U. S. A. 98 (2001) 10037–10041.
[75] J. Sánchez-Nieves, P. Ortega, M.A. Muñoz-Fernández, R. Gómez, F.J. de la Mata, Tetrahedron (2010) 9203–9213.
[76] F. Ritort, J. Phys. C 18 (2006) R531–R583.
[77] C.V. Bizarro, A. Alemany, F. Ritort, Nucleic Acids Res. 40 (2012) 6922–6935.
[78] J.M. Huguet, C.V. Bizarro, N. Forns, S.B. Smith, C. Bustamante, F. Ritort, PNAS 107 (2010) 15431–15436.
[79] J. Camunas-Soler, A. Alemany, F. Ritort, Science 335 (2017) 412–415.